

Protonic Ceramic Electrolysis Cells Design for NH₃ Synthesis

Subjects: Electrochemistry

Contributor: Hizkia Manuel Vieri, Moo-Chang Kim, Arash Badakhsh, Sun Hee Choi

The application of protonic ceramic electrolysis cells (PCECs) for ammonia (NH₃) synthesis has been evaluated over the past 14 years. While nitrogen (N₂) is the conventional fuel on the cathode side, various fuels such as methane (CH₄), hydrogen (H₂), and steam (H₂O) have been investigated for the oxygen evolution reaction (OER) on the anode side. Because H₂ is predominantly produced through CO₂-emitting methane reforming, H₂O has been the conventional carbon-free option thus far. Although the potential of utilizing H₂O and N₂ as fuels is considerable, studies exploring this specific combination remain limited.

Keywords: electrochemical ammonia synthesis ; protonic ceramic electrolysis cells ; hydrogen ; catalysts ; nitrogen reduction reaction

1. Introduction

Hydrogen (H₂) has considerable potential for energy storage. However, its low energy density poses challenges to storage and transport. One solution is to convert H₂ to ammonia (NH₃), where H₂ that is obtained from water electrolysis (i.e., green H₂) reacts with nitrogen (N₂) in the air to produce NH₃, which can be reversibly converted into H₂ and N₂ after transportation ^[1]. Currently, NH₃ is industrially produced using the Haber–Bosch process, which requires high pressure (100–200 bar) and temperature (300–400 °C) to activate the Fe-based catalysts ^{[2][3]}. Recent advancements include the hydrogenation of N₂ using Ru catalysts, which require milder reaction conditions ^[4].

However, the thermal approach for NH₃ synthesis remains expensive, as it requires a large centralized infrastructure and is energy-intensive, consuming approximately 485 kJ mol⁻¹ (approximately 2% of the global energy use per annum) ^[5]. Fertilizers Europe made conjectures about the decarbonization of the European NH₃ industry ^[6]. They proposed that approximately 10% of H₂ derived for NH₃ production in 2030 could possibly originate from renewable sources. Electrochemical NH₃ synthesis via N₂ reduction provides a relatively high efficiency of up to 20%, environmental compatibility with renewable sources (solar, tidal, and wind), on-site H⁺ generation from water oxidation, and adaptable reaction control ^[7]. This process converts sustainable electricity from sources such as wind power into NH₃ for use as a synthetic fuel or chemical feedstock ^{[8][9]}.

The operating conditions are classified into three types based on the temperature, namely, low (<100 °C), intermediate (200–500 °C), and high (>400 °C) temperature. High-temperature conditions enhance the catalytic activity and substantially increase the Faradaic efficiency in NH₃ synthesis. High-temperature NH₃ synthesis can be performed using proton-conducting electrolytes (PCEs) or oxygen-conducting electrolytes (OCEs). OCEs, while efficient, generally present slower rates of NH₃ production than PCEs ^[10]. This review focuses on NH₃ production in protonic ceramic electrolysis cells (PCECs), which operate at high temperatures (400–600 °C). As shown in **Figure 1**, the PCEC combines the nitrogen reduction reaction (NRR) with other electrochemical reactions that yield protons (H⁺), facilitating NH₃ production. Liu et al. briefly reviewed three primary PCEC configurations involving H₂, CH₄, and H₂O as proton (H⁺) sources. Although H₂O and N₂ have considerable potential as fuels, this specific combination has not been sufficiently investigated. Despite consuming substantially more electrical energy than the other configurations, using H₂O and N₂ directly to produce NH₃ is carbon-free and abundant in the feedstock ^[11]. This configuration couples the NRR with the oxygen evolution reaction (OER). High-temperature NH₃ synthesis has been extensively reviewed ^{[12][13][14][15][16]}. However, reviews of the specific PCEC configurations for NH₃ synthesis are limited. The unavailability of a comprehensive strategy for PCEC fabrication in a single study poses a considerable challenge for researchers aiming to develop PCECs customized for NH₃ synthesis.

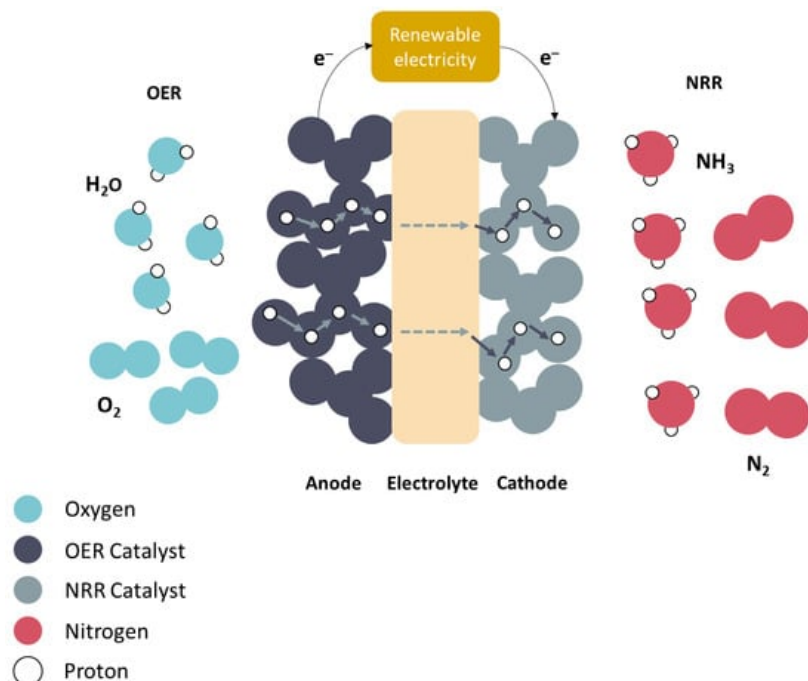


Figure 1. Schematic of the PCEC setup designed for NH_3 synthesis, wherein H_2O and N_2 are transformed into NH_3 .

The three essential components of a PCEC are an electrolyte, an anode, and a cathode (**Figure 1**). The electrolyte serves as an ion conductor that separates the electrodes and facilitates ion transport. The electrochemical reactions within the PCEC are non-spontaneous, implying that they do not occur naturally; an external influence, typically electricity, is necessary to drive the reactions [17].

Anode reaction

- At the anode, an electric current passes through water, thereby splitting water molecules into hydrogen (protons) and oxygen ions.
- Reaction: $2\text{H}_2\text{O} \rightarrow \text{O}_2 + 4\text{H}^+ + 4\text{e}^-$

Electron and proton transport:

- Electrons generated at the anode during water splitting are transported through an external electric circuit.
- Protons generated at the anode during water splitting are transported through the electrolyte [18].

Cathode reaction

- At the cathode, protons (H^+) from the anode and nitrogen atoms react to produce NH_3
- Reaction: $\text{N}_2 + 3\text{H}^+ + 3\text{e}^- \rightarrow \text{NH}_3$

2. PCEC Design Strategies

High-temperature cells such as solid oxide fuel cells (SOFCs) have been extensively designed [14]. However, selecting an appropriate design for each application is important because the cell performance strongly depends on the cathode, anode, and electrolyte materials. Medvedev discussed the influence of the design strategies on the performance of H_2 -producing PCECs [19]. However, PCEC design strategies for NH_3 synthesis are limited. This section describes the fabrication and design strategies for the electrolyte and electrodes.

2.1. Electrolyte Design Strategies

The electrolyte is considered the most important component of a PCEC, particularly in electrolyte-supported systems because it occupies the largest volume. BaCeO_3 and BaZrO_3 -based materials have been reported to be good protonic conductors [19]. Although BaCeO_3 exhibits high conductivity, BaZrO_3 provides better stability. Furthermore, Ce and Zr have been mixed with other dopants, such as Y and Yb, resulting in the well-known $\text{BaZr}_{0.4}\text{Ce}_{0.4}\text{Y}_{0.1}\text{Yb}_{0.1}\text{O}_{3-\delta}$ (BZCYb 4411) and $\text{BaZr}_{0.1}\text{Ce}_{0.7}\text{Y}_{0.1}\text{Yb}_{0.1}\text{O}_{3-\delta}$ (BZCYb 1711) electrolytes [20][21]. In general, a higher Ce content increases the proton

conductivity, whereas a higher Zr content increases the stability [22][23]. In a PCEC, the applied electrical current serves two potential pathways: proton and electron transfers. The primary objective of a PCEC is to facilitate the movement of protons (H^+) from the OER to the NRR sides, where they participate in hydrogen production. However, electron transfer, in which electrons move instead of protons, can be detrimental to the cell performance. This is because electron transfer reduces the Faradaic efficiency of the cell; particularly, a portion of the electrical energy is redirected to unintended reactions, leading to energy losses and potentially reducing the overall hydrogen production efficiency. Increasing the Ce content increases the protonic transference number and decreases the electron transference number. Therefore, BZCYYb 1711 is more suitable for PCECs than BZCYYb 4411 [24].

This discussion pertains to three distinct electrolyte forms: pellets, thin films, and columnar structures. Pellet-type electrolytes have been extensively used in fuel cells and batteries [25][26]. They are relatively easy to manufacture and integrate into PCEC stacks [27]. This method involves placing a few grams of electrolyte powder into a mold, which is typically cylindrical, and ultimately shaping it into a coin-like pellet. This conventional approach has resulted in considerable advancements in terms of electrolyte composition. The details of various pellet electrolytes developed thus far are listed in **Table 1**.

Table 1. Conductivities of proton-conducting electrolytes and their synthesis methods.

Electrolyte	Method	Conductivity ($S\ cm^{-1}$)	Thickness (mm)	Reference
$SrCe_{0.95}Yb_{0.05}O_{3-\delta}$	sol-gel	Unknown	1.5	[28]
$BaZr_{0.8-x-y}Ce_xNd_yY_{0.1}Yb_{0.1}O_{3-\delta}$	Pechini method	500 °C: 3.77×10^{-4}	0.8–1.5	[29]
$BaZr_{0.85}Y_{0.15}O_{3-\delta}$	hydrothermal process	600 °C: 2.5×10^{-3}	1.6	[30]

While the solid-state reaction is common for powder preparation, sol-gel or glycine nitrate processes are commonly employed to obtain finer particles and higher peak power densities [29]. The pellet electrolyte thickness is in the range of 0.8–1.6 mm (**Table 1**). Medvedev suggested that thin-film technology must be developed for the electrochemical synthesis of NH_3 [16]. With reference to the electrolyte properties, the thickness plays a crucial role in determining both the ohmic resistance and electron transport characteristics. Thicker electrolytes increase the ohmic resistance, whereas thinner electrolytes increase contact resistance at the electrolyte/electrode interface. In conventional electrolytes, the ohmic resistance tends to increase. This limitation can be effectively addressed using thin-film electrolytes [31]. Recent advancements in thin-film electrolytes for PCECs have been comprehensively presented in **Table 2**.

Table 2. Conductivities of thin-film electrolytes and their deposition/synthesis methods.

Electrolyte	Method	Conductivity ($S\ cm^{-1}$)	Thickness (μm)	Reference
$BaCe_{0.7}Zr_{0.1}Y_{0.2}$	co-precipitation solid-state reaction dip-coating	650 °C: 2.8×10^{-2}	~20	[32]
$BaCe_{0.8}Y_{0.2-x}Nd_xO_{3-\delta}$	citrate-nitrate combustion	350 °C: 8.5×10^{-3}	~20	[33]
$BaCe_{1-x}In_xO_{3-\delta}$	auto-combustion reaction	700 °C: 5×10^{-3}	20–25	[34]
$BaZr_{0.1}Ce_{0.7}Y_{0.1}Yb_{0.1}$	solid-state reaction	500 °C: 1.2×10^{-2}	10	[35]
$BaHf_{0.8}Yb_{0.2}O_{3-\delta}$	pulsed laser deposition (PLD)	500 °C: 2.5×10^{-3}	110	[35]
$BaZr_{0.1}Ce_{0.7}Y_{0.1}Yb_{0.1}$	solid-state reaction	500 °C: 1.3×10^{-2}	~10	[21]
$BaZr_{0.4}Ce_{0.4}Y_{0.1}Yb_{0.1}$	solid-state reaction	500 °C: 5.6×10^{-3}	~15	[20]
$BaZr_{0.2}Ce_{0.6}Y_{0.1}Yb_{0.1}O_{3-\delta}$	Pechini method inkjet printing	600 °C: 24.39	1	[36]
$BaCe_{0.5}Zr_{0.35}Y_{0.15}O_{3-\delta}$	citric nitrate method PLD	Unknown	2–4	[37]
$BaZr_{1-x-y}Ce_xY_yO_3$	ultrafast microwave-assisted sintering tape casting	Unknown	~12	[38]
$BaZr_{0.2}Ce_{0.6}Y_{0.2}O_3$	solid-state reaction spin coating	800 °C: 1×10^{-2}	~7	[39]

Electrolyte	Method	Conductivity (S cm ⁻¹)	Thickness (μm)	Reference
BaCe _{0.55} Zr _{0.3} Y _{0.15} O _{3-δ}	screen printing	Unknown	~2.5	[40]

The technological advancements in thin-film electrolytes are attributed to their reduced dimensions. Various deposition techniques, such as inkjet printing, pulsed layer deposition (PLD), tape casting, spin coating, and screen printing, are involved [36][37][38][39][40]. Screen printing and spin coating are known to be simple. However, considerable material wastage occurs, with a minimum thickness of approximately 10 μm. Furthermore, PLD, which is recognized for its effectiveness, requires complex operation and energy-intensive vacuum conditions. Inkjet printing offers the advantage of producing highly uniform surfaces with a minimum thickness of just 0.83 μm [36].

BaZr_{0.1}Ce_{0.7}Y_{0.1}Yb_{0.1} is an extensively investigated proton-conducting electrolyte, although some researchers have diverged, advocating other compositions as the most studied [21][32][34]. Some researchers have explored doping with elements such as Nd, Sc, In, and Hf, in addition to Y and Yb, to enhance the stability and sinterability of the electrolyte [21][30][31][33][35][41]. Ding et al. introduced a novel approach by ball milling, pelletizing, calcining, and crushing the pellets to produce a pure-phase powder on a relatively large scale (up to 4 kg per batch) [42]. Another approach involves combining all BZCYYb1711 nitrate precursors in deionized water, followed by the addition of a specific quantity of NaOH. NaOH reacts with nitrates and forms mixed metal hydroxides before calcination, which produce mixed metal oxides (perovskite). This mixture is washed and then subjected to a high-temperature solid-state reaction [41]. The conventional box furnace method at 1000–1500 °C with a ramp of 1–5 °C min⁻¹ is typically used for sintering. Spark plasma and microwave sintering have been examined for rapid high-temperature results, with the aim of matching or surpassing the performance of conventional sintering [34][43].

The previous discussion encompassed two distinct electrolyte types (**Figure 2**), namely, the planar type (pellet and thin film), which necessitates sealing agents for the reactor connection, and the tubular configuration, which operates seamlessly without requiring sealing. Columnar electrolytes can be fabricated by templating using plaster molds or by rolling a thin-film electrolyte. Notably, columnar electrolytes have been employed in SOFCs [44][45][46]. **Table 3** lists examples of columnar electrolyte utilization.

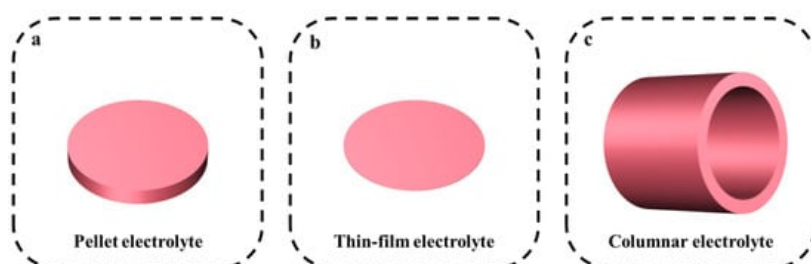


Figure 2. Illustration of (a) pellet, (b) thin-film, and (c) columnar electrolytes.

Table 3. Conductivities of columnar electrolytes and their deposition/synthesis method.

Electrolyte	Method	Conductivity	Reference
BaZr _{0.4} Ce _{0.4} Y _{0.15} Zn _{0.05} O ₃	solid-state reaction	Unknown	[47]
BaZr _{0.1} Ce _{0.7} Y _{0.1} Yb _{0.1}	solid-state reaction	Unknown	[48]

2.2. Electrode Design Strategies

In contrast to thermochemical catalysts, electrocatalysts must be pretreated to ensure that they can mechanically bond to the electrolyte while remaining catalytically active. In electrolyte-supported cells, the cathode and anode are deposited on opposite sides of the cell. The difference between the anode and cathode materials makes it necessary to specify the method that should be used to deposit them onto the electrolyte.

Recently, various conventional and ambient-condition deposition methods, such as the doctor blade method, drop coating, screen printing, tape casting, and spray coating, have been used to develop electrode materials for PCECs (**Table 4**). Although these methods are simple, the electrode thickness is controlled only through a randomized parameter, such as printing passes or number of drops. Therefore, many researchers have recently employed PLD to produce a smooth electrode surface and ensure good interfacial contact between the electrolyte and electrode [49].

Table 4. Deposition methods and electrode thickness in key research on OER and NRR catalysts.

Cathode	Deposition Method	Thickness (μm)	Reference
$\text{La}_{0.6}\text{Sr}_{0.4}\text{Co}_{0.2}\text{Fe}_{0.8}\text{O}_{3-\delta}$	Unknown	44	[50]
Ag	-	4	
Pt	-	8	
Fe	doctor blade	15–25	[51]
10-Fe-BCY	doctor blade	15–25	
0.5W-10Fe-BCY	doctor blade	15–25	
$\text{PrBa}_{0.5}\text{Sr}_{0.5}\text{Co}_{1.5}\text{Fe}_{0.5}\text{O}_{5+\delta}$	-	10–20	[23]
Ru–Ag/MgO	Unknown	-	[28]
Ni-BCYR	-	-	[52]
$\text{NdBa}_{0.5}\text{Sr}_{0.5}\text{Co}_{1.5}\text{Fe}_{0.5}\text{O}_{5+\delta}$ (NBSCF)-BZCYYb	drop coating	15	[53]
Pr_2NiO_4 -BZCY	screen printing	13	[54]
$\text{PrCo}_{0.05}\text{Ni}_{0.5}\text{O}_{3-\delta}$	tape casting	29	[55]
$\text{Ba}_{0.9}\text{Co}_{0.7}\text{Fe}_{0.2}\text{Nb}_{0.1}\text{O}_{3-\delta}$	screen printing	15	[56]
$\text{Pr}_{0.2}\text{Ba}_{0.2}\text{Sr}_{0.2}\text{La}_{0.2}\text{Ca}_{0.2}\text{CoO}_{3-\delta}$	spray coating	20	[57]
$\text{PrBa}_{0.5}\text{Sr}_{0.5}\text{Co}_{1.5}\text{Fe}_{0.5}\text{O}_{5+\delta}$	PLD	20	[58]
$\text{Gd}_{0.3}\text{Ca}_{2.7}\text{Co}_{3.82}\text{Cu}_{0.18}\text{O}_{9-\delta}$	screen printing	30	[59]

4. Current Progress

The NRR and OER have been studied extensively; the catalysts used for these reactions are summarized in Tables 5 and 6, respectively.

Table 5. Notable NRR catalysts in PCECs for NH_3 synthesis.

Cathode *	Electrolyte	NH_3 Production Rate [$\text{mol cm}^{-2} \text{s}^{-1}$] $\times 10^{-9}$	Thickness (μm)	Reference
$\text{La}_{0.6}\text{Sr}_{0.4}\text{Co}_{0.2}\text{Fe}_{0.8}\text{O}_{3-\delta}$	$\text{BaZr}_{0.8}\text{Y}_{0.2}\text{O}_{3-\delta}$	0.0850	44	[24]
Ag	$\text{BaZr}_{0.8}\text{Y}_{0.2}\text{O}_{3-\delta}$	0.0490	4	
Pt	$\text{BaZr}_{0.8}\text{Y}_{0.2}\text{O}_{3-\delta}$	<0.0010	8	
Fe	$\text{BaCe}_{0.9}\text{Y}_{0.1}\text{O}_{3-\delta}$	14.000	15–25	[26]
10-Fe-BCY	$\text{BaCe}_{0.9}\text{Y}_{0.1}\text{O}_{3-\delta}$	0.4200	15–25	
0.5W-10Fe-BCY	$\text{BaCe}_{0.9}\text{Y}_{0.1}\text{O}_{3-\delta}$	0.5700	15–25	
Ru–Ag/MgO	$\text{SrCe}_{0.95}\text{Yb}_{0.05}\text{O}_{3-\delta}$	0.0003	-	[41]
Ni-BCYR	$\text{BaCe}_{0.9}\text{Y}_{0.1}\text{O}_{3-\delta}$	0.0110	-	[63]

Based on Table 5, metallic catalysts evidently yield higher reaction rates. This could be attributed to two main factors. First, perovskite-based electrocatalysts may possibly be affected by degradation at the interface and thermal mismatch with the electrolyte, thus decreasing the performance [24]. Second, the electrochemical promotion of catalysis is more pronounced in pure metal catalysts with a higher effective double layer (S^*_{eff}) on their surfaces than in supported electrocatalysts [26]. However, pure metallic catalysts are typically expensive.

Ru is regarded as a suitable catalyst for thermochemical NH_3 synthesis because of its peak position on Skulason's volcano diagram, which shows that it requires a minimum potential for electrochemical NH_3 synthesis. It has also been reported to be an ultra-efficient electrocatalyst for the NRR, with a lower reduction potential than that of Fe [71–75]. However, Ag is a more cost-effective option because of its natural abundance. Although noble-metal-based electrocatalysts exhibit favorable activity, efficiency, and selectivity, their practical application is inhibited by their high cost and scarcity [27]. Consequently, extensive research has been conducted on transition-metal-based electrocatalysts for the NRR. The NH_3 synthesis rate of Pt catalysts can be primarily attributed to their strong HER activity [76,77]. At negative potentials, the surface of Pt nanoparticles tends to adsorb hydrogen atoms rather than nitrogen atoms, thus affecting the overall performance [78].

Table 6. Notable OER catalysts in PCECs for NH_3 synthesis.

Anode	Electrolyte	Current Density @1.3 V and 550 °C [A cm ⁻²]	Thickness (μm)	Reference
$Pr_{0.2}Ba_{0.2}Sr_{0.2}La_{0.2}Ca_{0.2}CoO_{3-\delta}$	$BaZr_{0.1}Ce_{0.7}Y_{0.1}Yb_{0.1}O_{3-\delta}$	-0.800	20	[68]
$PrBa_{0.5}Sr_{0.5}Co_{1.5}Fe_{0.5}O_{5+\delta}$	$BaZr_{0.4}Ce_{0.4}Y_{0.1}Yb_{0.1}O_{3-\delta}$	-1.059	20	[69]
$Gd_{0.3}Ca_{2.7}Co_{3.82}Cu_{0.18}O_{9-\delta}$	$BaZr_{0.1}Ce_{0.7}Y_{0.1}Yb_{0.1}O_{3-\delta}$	-1.241	30	[70]

Considering NH_3 -producing PCECs, most studies have only focused on the NRR, whereas the OER has been overlooked. The NH_3 synthesis reaction is typically performed at 475–600 °C [24]. Pei et al. briefly summarized the OER performance at a cell voltage of 1.3 V and operating temperature of 550 °C [67].

Currently, transition metals, particularly compounds based on Fe, Co, and Ni, have demonstrated remarkable catalytic activity for the OER [79]. A successful method to enhance the OER activity involves altering the surface electronic structure through the addition of supporting materials to the active metal (Fe, Co, or Ni). This strategy has attracted attention, particularly with reference to multi-metal materials such as high-entropy perovskites, because they provide numerous possibilities for modifying the characteristics and improving the catalytic performance [80].

Among multi-metal materials, Co-based double perovskite oxides are notable for their rapid ion diffusion and enhanced surface catalysis, resulting in high electrochemical performance in single cells [35,69,81]. Various studies have explored the application of OER catalysts in PCECs (Table 6). For example, $Gd_{0.3}Ca_{2.7}Co_{3.82}Cu_{0.18}O_{9-\delta}$ exhibits the highest current density owing to various factors, including abundant oxygen vacancies in the central Co–O layer of the $Ca_3Co_2O_3$ rock-salt subsystem, which alters the electronic charge carrier concentration. The needlelike grain morphology aids in the complex flow of the reaction components via triple conduction and open diffusion paths [70].

Despite the promising characteristics of Co-based double perovskite oxides, these high-entropy perovskite oxides have disadvantages such as instability, thermal mismatch, and high cost, which limit their widespread implementation [35,69,81,82]. Thermal mismatch occurs when the OER catalyst and electrolyte materials have different coefficients of thermal expansion (CTE). The CTE indicates the extent to which a material expands when exposed to changes in temperature. If the OER catalyst and electrolyte have significantly different CTE, they may expand at different rates as the temperature changes [83]. Therefore, catalysts with compatible mechanical properties need to be used.

References

1. Teichmann, D.; Stark, K.; Müller, K.; Zöttl, G.; Wasserscheid, P.; Arlt, W. Energy Storage in Residential and Commercial Buildings via Liquid Organic Hydrogen Carriers (LOHC). *Energy Environ. Sci.* 2012, 5, 9044–9054.
2. Kandemir, T.; Schuster, M.E.; Senyshyn, A.; Behrens, M.; Schlögl, R. The Haber–Bosch Process Revisited: On the Real Structure and Stability of “Ammonia Iron” under Working Conditions. *Angew. Chem. Int. Ed.* 2013, 52, 12723–12726.
3. Haber, F.; Rossignol, R. Le Über Die Technische Darstellung von Ammoniak Aus Den Elementen. *Zeitschrift für Elektrochemie und Angew. Phys. Chemie* 1913, 19, 53–72.
4. Aika, K.I.; Hori, H.; Ozaki, A. Activation of Nitrogen by Alkali Metal Promoted Transition Metal I. Ammonia Synthesis over Ruthenium Promoted by Alkali Metal. *J. Catal.* 1972, 27, 424–431.
5. IEA Ammonia Technology Roadmap. Available online: <https://www.iea.org/reports/ammonia-technology-roadmap> (accessed on 4 October 2023).
6. Brown, T. Feeding Life 2030: The Vision of Fertilizers Europe. Available online: <https://www.ammoniaenergy.org/articles/feeding-life-2030-the-vision-of-fertilizers-europe/> (accessed on 4 October 2023).
7. Shipman, M.A.; Symes, M.D. Recent Progress towards the Electrosynthesis of Ammonia from Sustainable Resources. *Catal. Today* 2017, 286, 57–68.
8. Foster, S.L.; Bakovic, S.I.P.; Duda, R.D.; Maheshwari, S.; Milton, R.D.; Minteer, S.D.; Janik, M.J.; Renner, J.N.; Greenlee, L.F. Catalysts for Nitrogen Reduction to Ammonia. *Nat. Catal.* 2018, 1, 490–500.
9. Jeerh, G.; Zhang, M.; Tao, S. Recent Progress in Ammonia Fuel Cells and Their Potential Applications. *J. Mater. Chem. A* 2021, 9, 727–752.
10. Gunduz, S.; Deka, D.J.; Ozkan, U.S. A Review of the Current Trends in High-Temperature Electrocatalytic Ammonia Production Using Solid Electrolytes. *J. Catal.* 2020, 387, 207–216.
11. Liu, F.; Ding, D.; Duan, C. Protonic Ceramic Electrochemical Cells for Synthesizing Sustainable Chemicals and Fuels. *Adv. Sci.* 2023, 10, e2206478.
12. Giddey, S.; Badwal, S.P.S.; Kulkarni, A. Review of Electrochemical Ammonia Production Technologies and Materials. *Int. J. Hydrogen Energy* 2013, 38, 14576–14594.
13. Garagounis, I.; Kyriakou, V.; Skodra, A.; Vasileiou, E.; Stoukides, M. Electrochemical Synthesis of Ammonia in Solid Electrolyte Cells. *Front. Energy Res.* 2014, 2, 1.
14. Wang, B.; Li, T.; Gong, F.; Othman, M.H.D.; Xiao, R. Ammonia as a Green Energy Carrier: Electrochemical Synthesis and Direct Ammonia Fuel Cell—A Comprehensive Review. *Fuel Process. Technol.* 2022, 235, 107380.
15. Juangsa, F.B.; Irhamna, A.R.; Aziz, M. Production of Ammonia as Potential Hydrogen Carrier: Review on Thermochemical and Electrochemical Processes. *Int. J. Hydrogen Energy* 2021, 46, 14455–14477.
16. Medvedev, D. Trends in Research and Development of Protonic Ceramic Electrolysis Cells. *Int. J. Hydrogen Energy* 2019, 44, 26711–26740.
17. Shen, H.; Choi, C.; Masa, J.; Li, X.; Qiu, J.; Jung, Y.; Sun, Z. Electrochemical Ammonia Synthesis: Mechanistic Understanding and Catalyst Design. *Chem* 2021, 7, 1708–1754.
18. Trivinho-Strixino, F.; Santos, J.S.; Souza Sikora, M. 3—Electrochemical Synthesis of Nanostructured Materials. In *Nanostructures*; Da Róz, A.L., Ferreira, M., de Lima Leite, F., Oliveira, O.N.B.T.-N., Eds.; William Andrew Publishing: Norwich, NY, USA, 2017; pp. 53–103. ISBN 978-0-323-49782-4.
19. Iwahara, H. Oxide-Ionic and Protonic Conductors Based on Perovskite-Type Oxides and Their Possible Applications. *Solid State Ionics* 1992, 52, 99–104.
20. Choi, S.; Kucharczyk, C.J.; Liang, Y.; Zhang, X.; Takeuchi, I.; Ji, H.I.; Haile, S.M. Exceptional Power Density and Stability at Intermediate Temperatures in Protonic Ceramic Fuel Cells. *Nat. Energy* 2018, 3, 202–210.
21. Liu, M.; Yang, L.; Wang, S.; Blinn, K.; Liu, M.; Liu, Z.; Cheng, Z. Enhanced Sulfur and Coking Tolerance of a Mixed Ion Conductor for SOFCs: BaZr_{0.1}Ce_{0.7}Y_{0.2}-XYbXO_{3-δ}. *Science* 2009, 326, 126–129.
22. Zhu, H.; Kee, R.J. Membrane Polarization in Mixed-Conducting Ceramic Fuel Cells and Electrolyzers. *Int. J. Hydrogen Energy* 2016, 41, 2931–2943.
23. Duan, C.; Kee, R.; Zhu, H.; Sullivan, N.; Zhu, L.; Bian, L.; Jennings, D.; O’Hayre, R. Highly Efficient Reversible Protonic Ceramic Electrochemical Cells for Power Generation and Fuel Production. *Nat. Energy* 2019, 4, 230–240.

24. Han, D.; Liu, X.; Bjørheim, T.S.; Uda, T. Yttrium-Doped Barium Zirconate-Cerate Solid Solution as Proton Conducting Electrolyte: Why Higher Cerium Concentration Leads to Better Performance for Fuel Cells and Electrolysis Cells. *Adv. Energy Mater.* 2021, 11, 2003149.
25. Zhu, J.; Li, X.L.; Wu, C.; Gao, J.; Xu, H.; Li, Y.; Guo, X.; Li, H.; Zhou, W. A Multilayer Ceramic Electrolyte for All-Solid-State Li Batteries. *Angew. Chemie Int. Ed.* 2021, 60, 3781–3790.
26. Brett, D.J.L.; Aguiar, P.; Clague, R.; Marquis, A.J.; Schöttl, S.; Simpson, R.; Brandon, N.P. Application of Infrared Thermal Imaging to the Study of Pellet Solid Oxide Fuel Cells. *J. Power Sources* 2007, 166, 112–119.
27. Feng, W.; Wu, W.; Jin, C.; Zhou, M.; Bian, W.; Tang, W.; Gomez, J.Y.; Boardman, R.; Ding, D. Exploring the Structural Uniformity and Integrity of Protonic Ceramic Thin Film Electrolyte Using Wet Powder Spraying. *J. Power Sources Adv.* 2021, 11, 100067.
28. Skodra, A.; Stoukides, M. Electrocatalytic Synthesis of Ammonia from Steam and Nitrogen at Atmospheric Pressure. *Solid State Ionics* 2009, 180, 1332–1336.
29. Yilmaz, S.; Kavici, B.; Ramakrishnan, P.; Celen, C.; Horri, B.A. Highly Conductive Cerium- and Neodymium-Doped Barium Zirconate Perovskites for Protonic Ceramic Fuel Cells. *Energies* 2023, 16, 4318.
30. François, M.; Lescure, V.; Heintz, O.; Combemale, L.; Demoisson, F.; Caboche, G. Synthesis of Y-Doped BaZrO₃ Proton Conducting Electrolyte Material by a Continuous Hydrothermal Process in Supercritical Conditions: Investigation of the Formation Mechanism and Electrochemical Performance. *Ceram. Int.* 2023, 49, 25344–25352.
31. Konwar, D.; Yoon, H.H. A Methane-Fueled SOFC Based on a Thin BaZr_{0.1}Ce_{0.7}Y_{0.1}Yb_{0.1}O_{3-δ} Electrolyte Film and a LaNi_{0.6}Co_{0.4}O₃ Anode Functional Layer. *J. Mater. Chem. A* 2016, 4, 5102–5106.
32. Fan, Z.; Cao, D.; Zhou, M.; Zhu, Z.; Chen, M.; Liu, J. Barium Cerate-Zirconate Electrolyte Powder Prepared by Carbonate Coprecipitation for High Performance Protonic Ceramic Fuel Cells. *Ceram. Int.* 2023, 49, 8524–8532.
33. Wang, S.; Shen, J.; Zhu, Z.; Wang, Z.; Cao, Y.; Guan, X.; Wang, Y.; Wei, Z.; Chen, M. Further Optimization of Barium Cerate Properties via Co-Doping Strategy for Potential Application as Proton-Conducting Solid Oxide Fuel Cell Electrolyte. *J. Power Sources* 2018, 387, 24–32.
34. Malešević, A.; Radojković, A.; Žunić, M.; Dapčević, A.; Perać, S.; Branković, Z.; Branković, G. Evaluation of Stability and Functionality of BaCe_{1-x}InxO_{3-δ} Electrolyte in a Wider Range of Indium Concentration. *J. Adv. Ceram.* 2022, 11, 443–453.
35. Kane, N.; Luo, Z.; Zhou, Y.; Ding, Y.; Weidenbach, A.; Zhang, W.; Liu, M. Durable and High-Performance Thin-Film BHfYb-Coated BZCYb Bilayer Electrolytes for Proton-Conducting Reversible Solid Oxide Cells. *ACS Appl. Mater. Interfaces* 2023, 15, 32395–32403.
36. Kim, Y.S.; Chang, W.; Jeong, H.J.; Kim, K.H.; Park, H.S.; Shim, J.H. High Performance of Protonic Ceramic Fuel Cells with 1-Mm-Thick Electrolytes Fabricated by Inkjet Printing. *Addit. Manuf.* 2023, 71, 103590.
37. Bae, K.; Lee, S.; Jang, D.Y.; Kim, H.J.; Lee, H.; Shin, D.; Son, J.W.; Shim, J.H. High-Performance Protonic Ceramic Fuel Cells with Thin-Film Yttrium-Doped Barium Cerate-Zirconate Electrolytes on Compositionally Gradient Anodes. *ACS Appl. Mater. Interfaces* 2016, 8, 9097–9103.
38. Kim, D.; Bae, K.T.; Kim, K.J.; Im, H.N.; Jang, S.; Oh, S.; Lee, S.W.; Shin, T.H.; Lee, K.T. High-Performance Protonic Ceramic Electrochemical Cells. *ACS Energy Lett.* 2022, 7, 2393–2400.
39. Lee, K.R.; Tseng, C.J.; Jang, S.C.; Lin, J.C.; Wang, K.W.; Chang, J.K.; Chen, T.C.; Lee, S.W. Fabrication of Anode-Supported Thin BCZY Electrolyte Protonic Fuel Cells Using NiO Sintering Aid. *Int. J. Hydrogen Energy* 2019, 44, 23784–23792.
40. Choi, S.M.; An, H.; Yoon, K.J.; Kim, B.K.; Lee, H.W.; Son, J.W.; Kim, H.; Shin, D.; Ji, H.I.; Lee, J.H. Electrochemical Analysis of High-Performance Protonic Ceramic Fuel Cells Based on a Columnar-Structured Thin Electrolyte. *Appl. Energy* 2019, 233–234, 29–36.
41. Zhong, Z.; Li, Z.; Li, J.; Guo, X.; Hu, Q.; Feng, Y.; Sun, H. A Facile Method to Synthesize BaZr_{0.1}Ce_{0.7}Y_{0.1}Yb_{0.1}O_{3-δ} (BZCYb) Nanopowders for the Application on Highly Conductive Proton-Conducting Electrolytes. *Int. J. Hydrogen Energy* 2022, 47, 40054–40066.
42. Wang, M.; Wu, W.; Lin, Y.; Tang, W.; Gao, G.; Li, H.; Stewart, F.F.; Wang, L.; Yang, Y.; Ding, D. Improved Solid-State Reaction Method for Scaled-Up Synthesis of Ceramic Proton-Conducting Electrolyte Materials. *ACS Appl. Energy Mater.* 2023, 6, 8316–8326.
43. Sari, S.N.; Nieroda, P.; Pasierb, P. The BaCeO₃-Based Composite Protonic Conductors Prepared by Spark Plasma Sintering (SPS) and Free-Sintering Methods. *Int. J. Hydrogen Energy* 2023, 48, 29748–29758.

44. Timurkutluk, C.; Timurkutluk, B.; Kaplan, Y. Experimental Optimization of the Fabrication Parameters for Anode-Supported Micro-Tubular Solid Oxide Fuel Cells. *Int. J. Hydrogen Energy* 2020, 45, 23294–23309.
45. Ren, C.; Xu, P.; Zhang, Y.; Liu, T. Understanding the Polymer Binder Effect on the Microstructure and Performance of Micro-Tubular Solid Oxide Fuel Cells with Continuously Graded Pores Fabricated by the Phase Inversion Method. *Appl. Surf. Sci.* 2023, 612, 155928.
46. Sun, H.; Zhang, S.; Li, C.; Rainwater, B.; Liu, Y.; Zhang, L.; Zhang, Y.; Li, C.; Liu, M. Atmospheric Plasma-Sprayed BaZr_{0.1}Ce_{0.7}Y_{0.1}Yb_{0.1}O_{3-δ} (BZCYYb) Electrolyte Membranes for Intermediate-Temperature Solid Oxide Fuel Cells. *Ceram. Int.* 2016, 42, 19231–19236.
47. Xiao, Y.; Wang, M.; Bao, D.; Wang, Z.; Jin, F.; Wang, Y.; He, T. Performance of Fuel Electrode-Supported Tubular Protonic Ceramic Cells Prepared through Slip Casting and Dip-Coating Methods. *Catalysts* 2023, 13, 182.
48. Hou, M.; Zhu, F.; Liu, Y.; Chen, Y. A High-Performance Fuel Electrode-Supported Tubular Protonic Ceramic Electrochemical Cell. *J. Eur. Ceram. Soc.* 2023, 43, 6200–6207.
49. Oneill, B.J.; Jackson, D.H.K.; Lee, J.; Canlas, C.; Stair, P.C.; Marshall, C.L.; Elam, J.W.; Kuech, T.F.; Dumesic, J.A.; Huber, G.W. Catalyst Design with Atomic Layer Deposition. *ACS Catal.* 2015, 5, 1804–1825.
50. Yun, D.S.; Joo, J.H.; Yu, J.H.; Yoon, H.C.; Kim, J.N.; Yoo, C.Y. Electrochemical Ammonia Synthesis from Steam and Nitrogen Using Proton Conducting Yttrium Doped Barium Zirconate Electrolyte with Silver, Platinum, and Lanthanum Strontium Cobalt Ferrite Electrocatalyst. *J. Power Sources* 2015, 284, 245–251.
51. Li, C.I.; Matsuo, H.; Otomo, J. Effective Electrode Design and the Reaction Mechanism for Electrochemical Promotion of Ammonia Synthesis Using Fe-Based Electrode Catalysts. *Sustain. Energy Fuels* 2021, 5, 188–198.
52. Kosaka, F.; Nakamura, T.; Otomo, J. Electrochemical Ammonia Synthesis Using Mixed Protonic-Electronic Conducting Cathodes with Exsolved Ru-Nanoparticles in Proton Conducting Electrolysis Cells. *J. Electrochem. Soc.* 2017, 164, F1323–F1330.
53. Kim, J.; Jun, A.; Gwon, O.; Yoo, S.; Liu, M.; Shin, J.; Lim, T.H.; Kim, G. Hybrid-Solid Oxide Electrolysis Cell: A New Strategy for Efficient Hydrogen Production. *Nano Energy* 2018, 44, 121–126.
54. Li, W.; Guan, B.; Ma, L.; Hu, S.; Zhang, N.; Liu, X. High Performing Triple-Conductive Pr₂NiO_{4+δ} Anode for Proton-Conducting Steam Solid Oxide Electrolysis Cell. *J. Mater. Chem. A* 2018, 6, 18057–18066.
55. Ding, H.; Wu, W.; Jiang, C.; Ding, Y.; Bian, W.; Hu, B.; Singh, P.; Orme, C.J.; Wang, L.; Zhang, Y.; et al. Self-Sustainable Protonic Ceramic Electrochemical Cells Using a Triple Conducting Electrode for Hydrogen and Power Production. *Nat. Commun.* 2020, 11, 1907.
56. Pei, K.; Zhou, Y.; Xu, K.; Zhang, H.; Ding, Y.; Zhao, B.; Yuan, W.; Sasaki, K.; Choi, Y.M.; Chen, Y.; et al. Surface Restructuring of a Perovskite-Type Air Electrode for Reversible Protonic Ceramic Electrochemical Cells. *Nat. Commun.* 2022, 13, 2207.
57. He, F.; Zhou, Y.; Hu, T.; Xu, Y.; Hou, M.; Zhu, F.; Liu, D.; Zhang, H.; Xu, K.; Liu, M.; et al. An Efficient High-Entropy Perovskite-Type Air Electrode for Reversible Oxygen Reduction and Water Splitting in Protonic Ceramic Cells. *Adv. Mater.* 2023, 35, e2209469.
58. Choi, S.; Davenport, T.C.; Haile, S.M. Protonic Ceramic Electrochemical Cells for Hydrogen Production and Electricity Generation: Exceptional Reversibility, Stability, and Demonstrated Faradaic Efficiency. *Energy Environ. Sci.* 2019, 12, 206–215.
59. Saqib, M.; Choi, I.G.; Bae, H.; Park, K.; Shin, J.S.; Kim, Y.D.; Lee, J.I.; Jo, M.; Kim, Y.C.; Lee, K.S.; et al. Transition from Perovskite to Misfit-Layered Structure Materials: A Highly Oxygen Deficient and Stable Oxygen Electrode Catalyst. *Energy Environ. Sci.* 2021, 14, 2472–2484.